Combination Efficacy of *Astragalus membranaceus* and *Curcuma wenyujin* at Different Stages of Tumor Progression in an Imageable Orthotopic Nude Mouse Model of Metastatic Human Ovarian Cancer Expressing Red Fluorescent Protein

GANG YIN[1], DECAI TANG[1], JIANGUO DAI[1], MIN LIU[1], MIANHUA WU[1], YU SUN[2], ZHIJIAN YANG[2,3], ROBERT M. HOFFMAN[3,4], LIN LI[1], SHUO ZHANG[1] and XIUXIA GUO[1]

[1]*Nanjing University of Chinese Medicine, Nanjing, P.R. China;*
[2]*Origin Biosciences Inc., Nanjing, Jiangsu, P.R. China;*
[3]*AntiCancer, Inc., San Diego, CA, U.S.A.;*
[4]*Department of Surgery, University of California, San Diego, CA, U.S.A.*

Abstract. *Background/Aim. The present study determined the efficacy of extracts of Astragalus membranaceus (AM) and Curcuma wenyujin (CW), a traditional Chinese medicine herbal mixture, at different tumor stages of an orthotopic nude mouse model of human ovarian cancer expressing red fluorescent protein. Materials and Methods: The tumor-bearing mice were treated with cisplatinum (CDDP), AM, CW, or a combination of AM and CW in each of three tumor stages, using the same regimen. Group 1 received saline as negative control. Group 2 received CDDP i.p. as positive control with a dose of 2 mg/kg, every three days. Group 3 received AM daily via oral gavage, at a dose of 9120 mg/kg. Group 4 received CW daily via oral gavage, at a dose of 4560 mg/kg. Groups 5, 6 and 7 received combinations of AM and CW daily via oral gavage at low (AM, 2280 mg/kg; CW, 1140 mg/kg), medium (AM, 4560 mg/kg; CW 2280 mg/kg), and high (AM, 9120 mg/kg; CW, 4560 mg/kg) doses. The expression of angiogenesis- and apoptosis-related genes in the tumors were analyzed by immunohistochemistry for matrix metalloproteinase 2 (MMP-2), vascular endothelial growth factor (VEGF) fibroblast growth factor 2 (FGF-2), B-cell lymphoma 2 (Bcl-2) and cyclooxygenase 2 (Cox-2), and by polymerase chain reaction for MMP-2, FGF-2 and Bcl-2. Results: CDDP, AM, and its combination with CW-induced significant growth inhibition of Stage I tumors. Strong efficacy of the combination of AM and CW at high dose was observed. Monotherapy with CDDP, AM, CW, and the combination treatments did not significantly inhibit Stage II and III tumors. The expression of MMP-2, VEGF, FGF-2, and Cox-2 was significantly reduced in Stage I tumors treated with AM, CW, and their combination, suggesting a possible role of these angiogenesis- and apoptosis-related genes in the observed efficacy of the agents tested. Conclusion: This study is the first report on the efficacy of anticancer agents at different stages of ovarian cancer in an orthotopic mouse model. As the tumor progressed, it became treatment-resistant, similar to the clinical situation, further demonstrating the utility of the model and the need for agents acrtive in advanced-stage ovarian cancer.*

Correspondence to: Decai Tang, Nanjing University of Chinese Medicine, 138 Xianlin Avenue, Nanjing, Jiangsu 210023, P.R. China. E-mail: talknow@njucm.edu.cn

Key Words: *Astragalus membranaceus*, *Curcuma wenyujin*, ovarian cancer, red fluorescent protein, orthotopic, nude mice, tumor progression, metastasis.

In 1993, we reported the first orthotopic transplant model for human ovarian cancer. Histologically-intact patient specimens of ovarian cancer were transplanted by microsurgical techniques under the capsule of the nude-mouse ovary. The human tumors grew locally and gave rise to a patient-like metastatic pattern, including the parietal peritoneum, colon, omentum, and ascites (1, 2).

We subsequently developed a green fluorescent protein (GFP)-expressing orthotopic metastatic nude-mouse model of the human ovarian cancer cell line SKOV3-GFP, enabling noninvasive imaging of tumor progression and metastasis (3).

The present study investigated the efficacy of a traditional Chinese medicinal herbal mixture on the various stages of an orthotopic nude-mouse model of human ovarian cancer expressing red fluorescent protein (RFP), enabling noninvasive imaging of tumor progression (3-5).

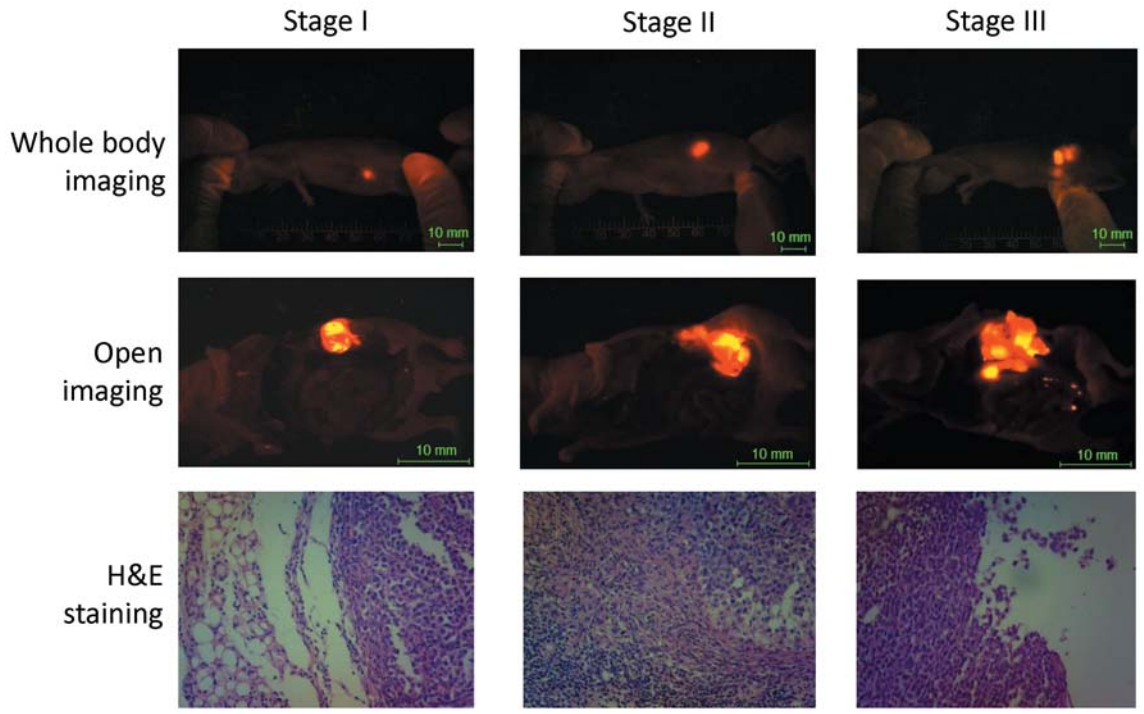

Figure 1. *Staging of orthotopic mouse model of human ovarian cancer. In vivo fluorescence imaging and histological examination were performed to stage the orthotopic human HO-8910-RFP ovarian tumor mouse model. Panels depict whole-body noninvasive fluorescence imaging, open imaging at autopsy and H&E staining of the orthotopic ovarian tumor in a representative mouse at each of three stages.*

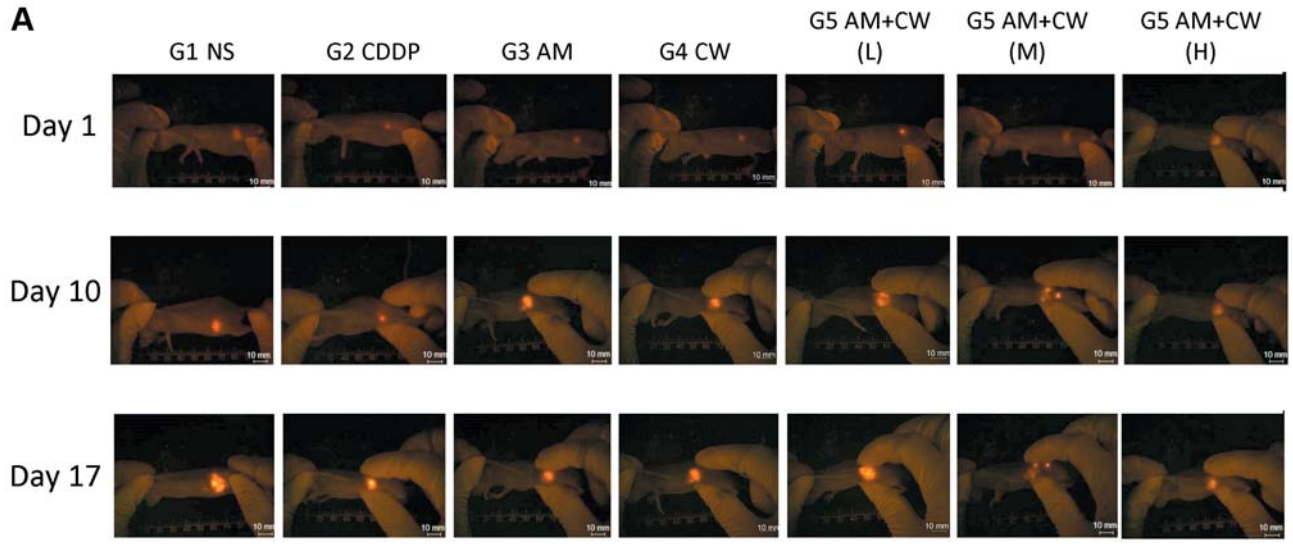

Figure 2. *Continued*

The dried root of *Astragalus membranaceus* (Fischer) Bge. var. mongholicus (Bge.) Hsiao (AM) is a traditional Chinese medicine (TCM). AM is frequently prescribed in many formulations and has been reported to possess diverse biological activities, including cardioprotective (6, 7), immunomodulatory (8, 9), anti-inflammatory and anti-cancer (10, 11). AM had significant growth-inhibitory, pro-apoptotic and angiogenesis suppression on colon, breast, hepatocellular, gastric, prostate and cervical human cancer cells *in vitro* (12-18). In addition, AM inhibited growth of colon and breast cancer *in vivo* (12, 19).

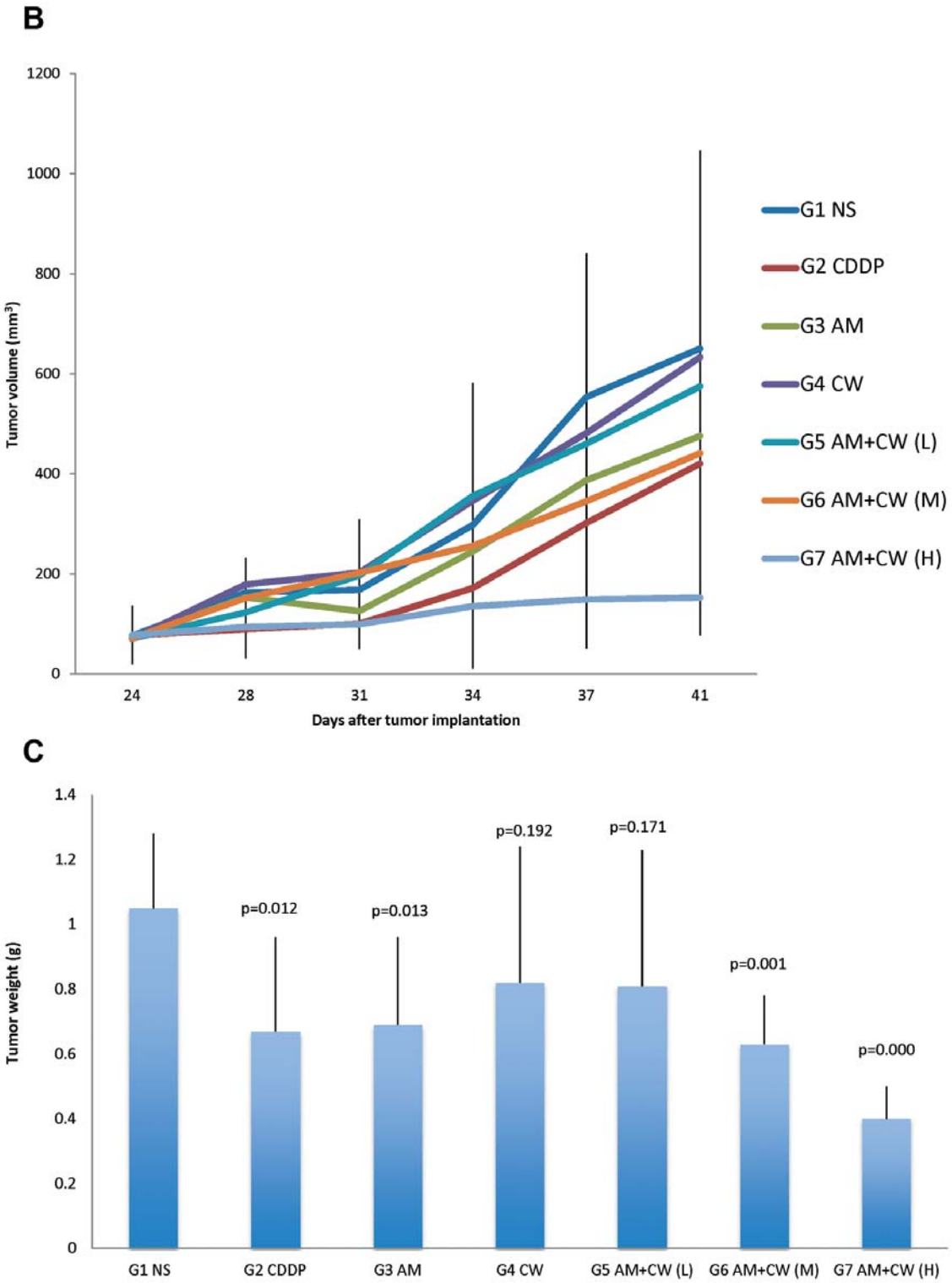

Figure 2. *Efficacy of Astragalus membranaceus (AM) and Curcuma wenyujin (CW) on Stage I tumor growth in the orthotopic human HO-8910-RFP ovarian cancer mouse model. Tumor growth was monitored and quantified by real-time noninvasive whole-body fluorescence imaging. Tumor was dissected and final tumor weight was determined at autopsy. A: Sequential in vivo whole-body fluorescence imaging of tumor on day 0, 10 and 17 after treatment initiation in mice treated with normal saline (NS), cisplatinum (CDDP), AM, CW, or low- (L), medium- (M), or high-dose (H) AM+CW. B: Tumor growth curves for mice treated with NS, CDDP, AM, CW and their combination. C: Final tumor weights at the end of the study in the mice of control and treated groups.*

Table 1A. *Efficacy on metastasis of Stage I tumors*.

Group	No. of animals in group	Total MI	*p*-Value	L.N. MI	*p*-Value	Pancreatic MI	*p*-Value
G1	8	3		3		1	
G2	8	0	*p*>0.05	0	*p*>0.05	0	*p*>0.05
G3	8	0	*p*>0.05	0	*p*>0.05	0	*p*>0.05
G4	8	0	*p*>0.05	0	*p*>0.05	0	*p*>0.05
G5	8	0	*p*>0.05	0	*p*>0.05	0	*p*>0.05
G6	8	1	*p*>0.05	0	*p*>0.05	1	*p*>0.05
G7	8	0	p>0.05	0	p>0.05	0	p>0.05

MI: Metastasis incidence; L.N.: Lymph node

Table 1B. *Efficacy on metastasis of Stage II tumors*.

Group	No. of animals in group	Total MI	*p*-Value	L.N. MI	*p*-Value	Pancreatic MI	*p*-Value
G1	8	3		3		0	
G2	8	0	*p*>0.05	0	*p*>0.05	0	*p*>0.05
G3	8	0	*p*>0.05	0	*p*>0.05	0	*p*>0.05
G4	8	3	*p*>0.05	3	*p*>0.05	2	*p*>0.05
G5	8	2	*p*>0.05	2	*p*>0.05	2	*p*>0.05
G6	8	1	*p*>0.05	0	*p*>0.05	1	*p*>0.05
G7	8	2	*p*>0.05	2	*p*>0.05	0	*p*>0.05

MI: Metastasis incidence; L.N.: Lymph node

Table 1C. *Efficacy on metastasis of Stage III tumors*.

Group	No. of animals in group	Total MI	*p*-Value	L.N. MI	*p*-Value	Pancreatic MI	*p*-Value	Ascites MI	*p*-Value
G1	8	7		7		2		7	
G2	8	3	*p*>0.05	3	*p*>0.05	0	*p*>0.05	1	*p*>0.05
G3	8	4	*p*>0.05	3	*p*>0.05	0	*p*>0.05	1	*p*>0.05
G4	8	2	*p*>0.05	0	*p*>0.05	0	*p*>0.05	2	*p*>0.05
G5	8	3	*p*>0.05	1	*p*>0.05	0	*p*>0.05	2	*p*>0.05
G6	8	3	*p*>0.05	6	*p*>0.05	0	*p*>0.05	2	*p*>0.05
G7	8	3	p>0.05	2	p>0.05	1	p>0.05	2	p>0.05

MI: Metastasis incidence; L.N.: Lymph node

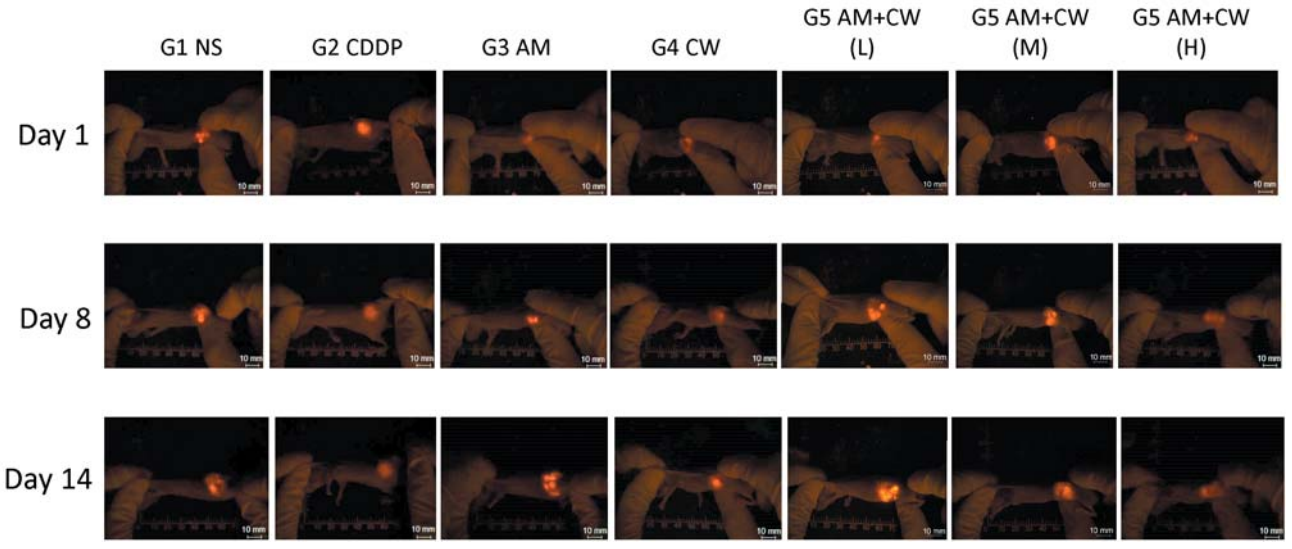

Figure 3. *Continued*

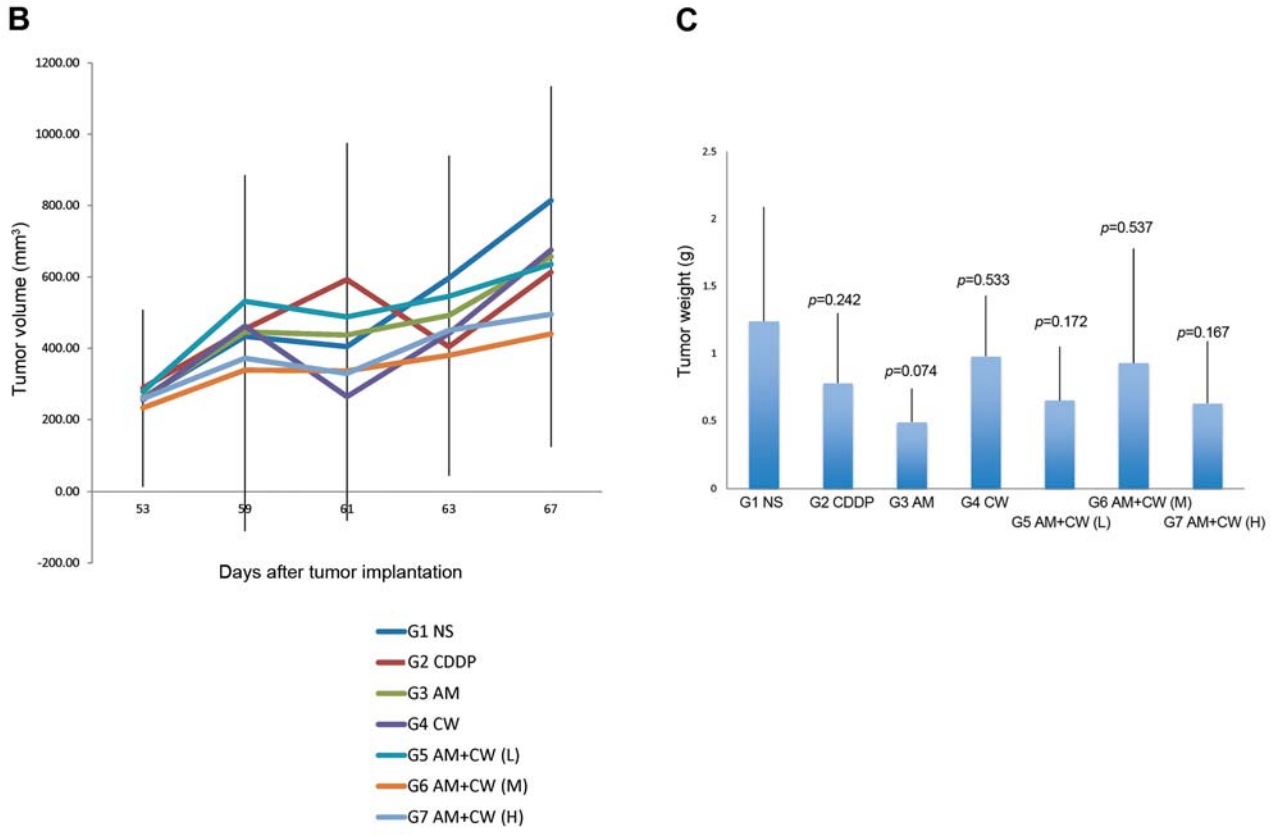

Figure 3. *Efficacy of Astragalus membranaceus (AM) and Curcuma wenyujin (CW) on Stage II tumor growth in the orthotopic human HO-8910-RFP ovarian cancer mouse model. Tumor growth was monitored and quantified by real-time noninvasive whole-body fluorescence imaging. Tumor was dissected and final tumor weight was determined at autopsy. A: Sequential in vivo whole-body fluorescence imaging of tumor on day 0, 8 and 14 in mice treated with normal saline (NS), cisplatinum (CDDP), AM, CW, or low- (L), medium- (M), or high-dose (H) AM+CW. B: Tumor growth curves for mice treated with NS, CDDP, AM, CW and their combination. C: Final tumor weights at the end of the study in the mice of control and treated groups.*

Curcuma wenyujin Y.H. Chen et C. Ling (CW), a widely prescribed TCM in clinical cancer therapy, also has antimicrobial (20) antiinflammatory (21, 22), and antiproliferative acitivies (20, 23-26). CW significantly inhibited uterine-cervical, prostate, gastric and breast cancer cell proliferation *in vitro*, and inhibited tumor growth in mouse models (27-30).

We previously reported proliferation inhibition and apoptosis induction by CW in HO-8910 ovarian cancer cells *in vitro* (31). Previous *in vivo* studies on AM and CW were performed on subcutaneous xenograft tumor models, which have limited clinical relevance.

In the present report, tumor progression in an orthotopic mouse model of ovarian cancer was classified into three stages by *in vivo* fluorescence imaging and histology in order to minic the clinical situation. The efficacy of AM and CW on each stage of tumor progression was evaluated. Expression of angiogenesis- and apoptosis-related genes in the tumors treated with AM and CW was evaluated to determine the mechanism of action of these herbal agents.

Materials and Methods

Cell culture. The HO-8910 human ovarian cancer cell line expressing RFP (HO-8910-RFP) (AntiCancer, Inc., San Diego, CA, USA), was cultured in RPMI-1640 medium (Gibco Life Technologies, Grand Island, NY, USA) supplemented with 10% heat-inactivated fetal bovine serum (FBS) (Hyclone, Logan, UT, USA) at –37˚C in an atmosphere of 5% CO_2 and saturated humidity. The medium was supplemented with penicillin/streptomycin (Gibco Life Technologies).

Animal care. BALB/C female nude mice (n=168), aged 4-6 weeks, weighing 20-25 g, were purchased from the Shanghai Laboratory Animal Center (SLAC) (Shanghai, China). All mice were maintained in a HEPA-filtered environment at 24-25˚C and humidity was maintained at 50-60%. All animals were fed with autoclaved laboratory rodent diet. Animal experiments were approved by the Animal Committee of Nanjing Origin Biosciences (Nanjing, China) (OR1305).

Orthotopic mouse model. An orthotopic mouse model of HO-8910-RFP human ovarian cancer cell line was used for the present study (1-3). HO-8910-RFP stock tumor was established by subcutaneously injecting

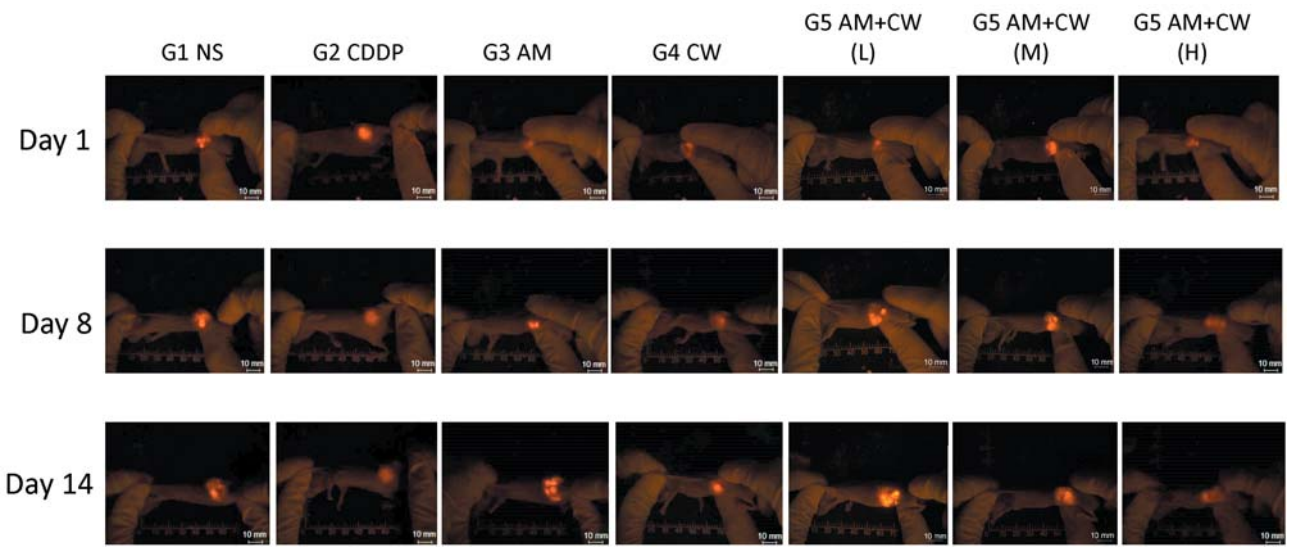

Figure 4. *Continued*

HO-8910-RFP cells (5×10^6) into the flank of nude in mice. Ovarian tumors grown s.c. in nude mice were harvested in the exponential growth phase and resected under aseptic conditions. Strong RFP expression of the HO-8910-RFP tumor tissue was confirmed by fluorescence microscopy. Necrotic tissues were removed and viable tissues were cut with scissors and minced into 1 mm^3 pieces. Animals were anesthetized by injection of a solution of 50 mg/ml ketamine, 38 mg/ml xylazine, and 1.2 mg/ml acepromazine maleate (0.02 ml). The surgical orthotopic implantation (SOI) method followed our published procedures (1-3, 32). An incision approximately 1 cm long was made in the right lower abdomen of the nude mouse below the kidney using sterile scissors. The ovary was exposed and the capsule of the ovary was carefully opened. One ovarian tumor fragment was sutured to the ovary with 8-0 surgical sutures. The abdomen was closed in layers with sterile 5-0 surgical sutures. All surgical procedures and animal manipulations were conducted under aseptic conditions in a HEPA-filtered laminar-flow hood under a surgical microscope (Model YZ20P5, Shanghai Precision Instruments, Shanghai, China).

In vivo fluorescence imaging. A fluorescence stereo microscope (MZ650; Nanjing Optic Instrument Inc., Nanjing, China) equipped with D510 longpass and HQ600/50 bandpass emission filters (Chroma Technology, Brattleboro, VT, USA) and a cooled color charge-coupled device camera (QImaging, Surry, BC, Canada) were used. Selective excitation of RFP was produced through an illuminator equipped with HQ470/40 and HQ540/40 excitation bandpass filters (Chroma Technology, Brattleboro, VT, USA). Images were processed and analyzed with the use of IMAGE PRO Plus 6.0 software (Media Cybernetics, Silver Spring, MD, USA).

Staging of orthotopic mouse model of human ovarian cancer. Whole-body fluorescence imaging was performed on tumor-bearing mice weekly after tumor implantation to observe tumor growth and metastasis. Each week, three mice were sacrificed for open fluorescence imaging and then primary tumor and metastases were collected for histological examination. An experienced gynecological pathologist performed the histological evaluation. Three stages of tumor progression in mice were classified with reference to the criteria of the International Federation of Gynecologists and Obstetricians (FIGO) (33, 34). Stage I tumors were those growing in the primary site and not outside the capsule of the ovary; Stage II tumors were those growing in the primary site and through the capsule of the ovary, but had not spread to surrounding tissues; Stage III tumors were those growing in multiple sites and which had metastasized to other pelvic tissues and abdominal lymph nodes.

Treatment. Extracts from AM and CW used in the study were supplied by the Nanjing University of Chinese Medicine and kept at 4˚C until use. AM and CW extracts were dissolved and diluted with distilled water before administration.

Treatment of Stage I, II, and III tumors was initiated on the day determined by staging of the tumor model. For the treatments at each stage, 56 mice were randomized into seven groups of eight mice each after tumor size and progression were confirmed by fluorescence imaging for the corresponding stage. The mice at each stage were treated with the same regimen. Group 1 served as the negative control and received daily saline (NS) *via* oral gavage at the same dosing volume as the treated animals. Group 2 served as the positive control and received cisplatinum (CDDP) *i.p.* at a dose of 2 mg/kg every three days. Group 3 received AM, *via* oral gavage, at a dose of 9120 mg/kg. Group 4 received CW, *via* oral gavage, at a dose of 4560 mg/kg. Group 5 received the combination of AM and CW, *via* oral gavage, at a low dose (AM, 2280 mg/kg; CW, 1140 mg/kg). Group 6 received the combination, *via* oral gavage, at a medium dose (AM, 4560 mg/kg; CW 2280 mg/kg). Group 7 received the combination, *via* oral gavage, at a high dose (AM, 9120 mg/kg; CW, 4560 mg/kg). Dosing for AM and CW was performed daily until the end of the study. Each animal was examined daily for clinical signs during the treatment period. The body weight for each animal was measured twice a week to monitor toxicity. At the end of the study, tumors were dissected and final tumor weights were determined for each animal.

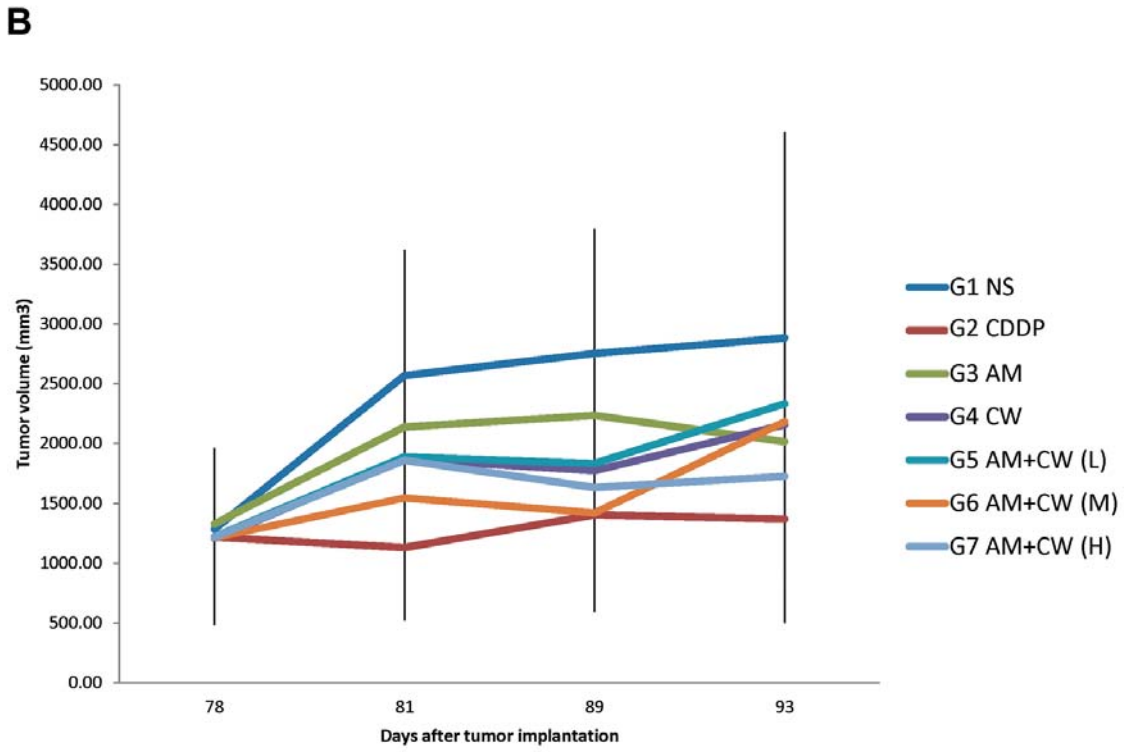

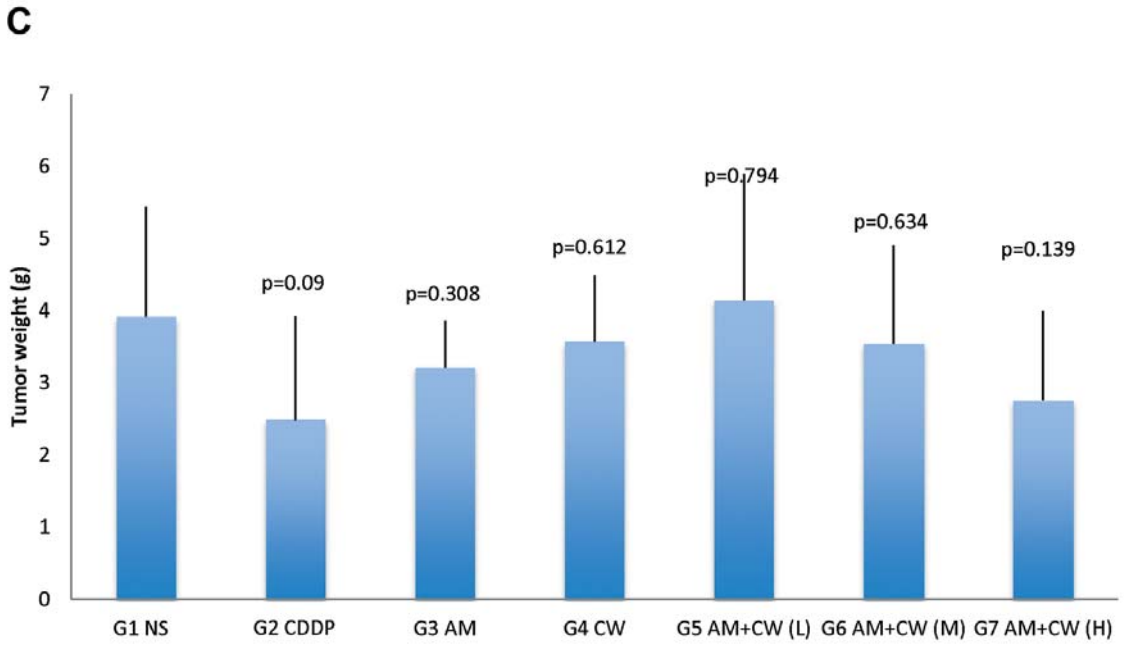

Figure 4. *Efficacy of Astragalus membranaceus (AM) and Curcuma wenyujin (CW) on Stage III tumor growth in the orthotopic human HO-8910-RFP ovarian cancer mouse model. Tumor growth was monitored and quantified by real-time whole-body fluorescence imaging. Tumor was dissected and final tumor weight was determined at autopsy. A: Sequential in vivo non-invasive whole-body fluorescence imaging of tumor on day 0, 11 and 15 after treatment initiation in mice treated with normal saline (NS), cisplatinum (CDDP), AM, CW, or low- (L), medium- (M), or high-dose (H) AM+CW. B: Tumor growth curves for mice treated with NS, CDDP, AM, CW and their combination. C: Final tumor weights at the end of the study in the mice of control and treated groups.*

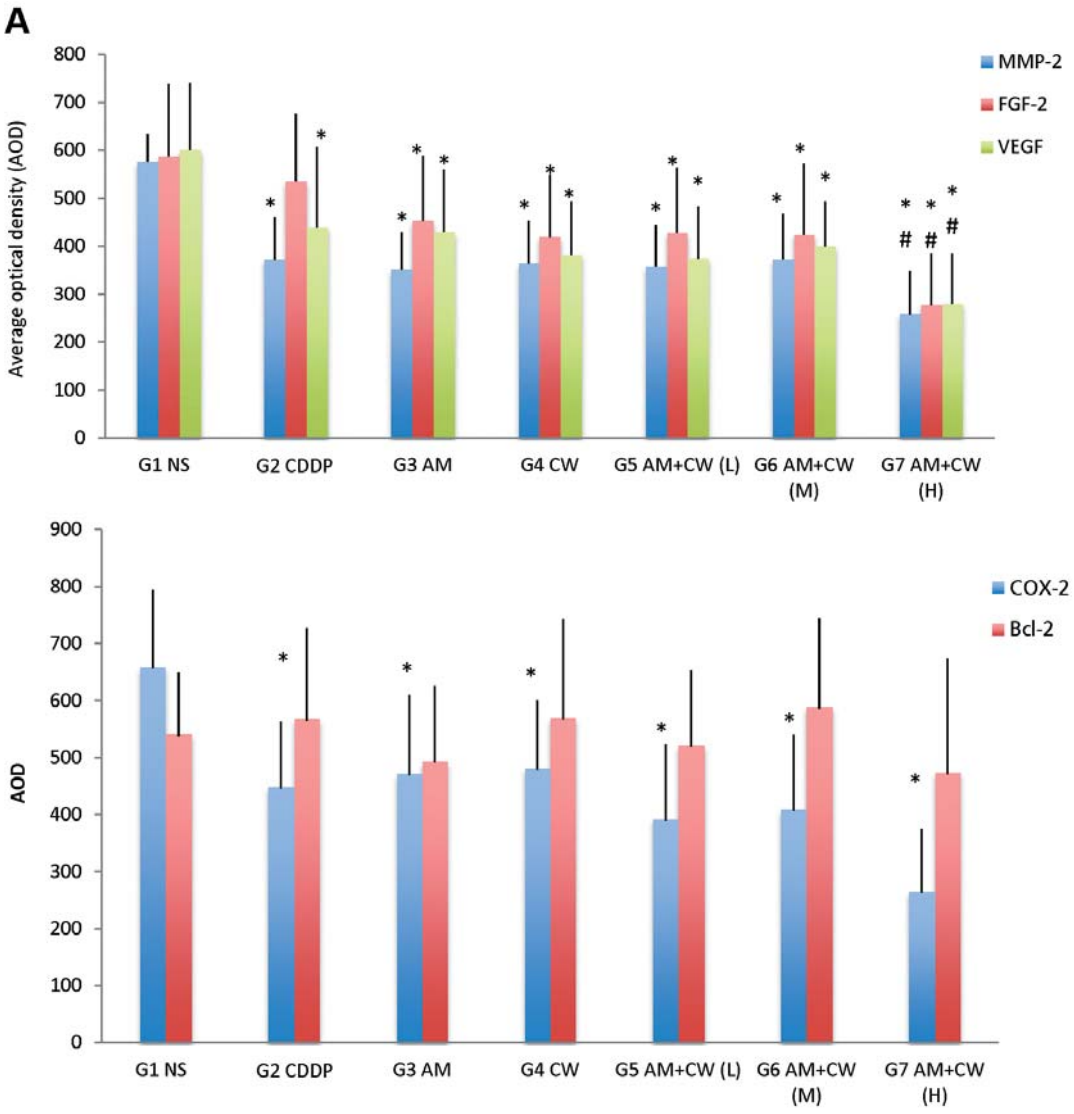

Figure 5. *Continued*

Immunohistochemistry. Immunohistochemistry was used to detect protein expression of matrix metalloproteinase 2 (MMP-2), vascular endothelial growth factor (VEGF), fibroblast growth factor 2 (FGF-2), B-cell lymphoma 2 (Bcl-2) and cyclooxygenase 2 (Cox-2) in the tumor tissue samples. The tissue sections were incubated with primary antibodies against MMP-2, VEGF, FGF-2, Bcl-2 and Cox-2 (BD Biosciences, San Diego, CA, USA), respectively, overnight at 4˚C after permeabilization with a solution of 0.1% sodium citrate and 0.1%Triton X100 and blocking with 10% rabbit serum. After washing in phosphate buffered saline, the slices were incubated with horseradish peroxidase-labeled secondary antibody (1:200; Maixin BioTech Co., Ltd., Fuzhou, China) for 30 min at room temperature. After color development using diaminobenzidine (Maixin BioTech Co., Ltd), the slices were counterstained with hematoxylin and mounted with a neutral resin medium. The slides were viewed at ×400 magnification and positive cells were recognized by the appearance of brown staining. The expression level was quantified by the average optical density (AOD) of the positive cells in five fields per sample with ImagePro Plus 6.0 software. (Media Cybernetics, Silver Spring, MD, USA).

Reverse transcription-polymerase chain reaction (RT-PCR) analysis. RT-PCR was used to analyze the mRNA expression of MMP-2, Bcl-2 and FGF-2 in the tumor tissue samples. Total RNA extraction and purification were performed with an RNA extraction kit (Promega, Madison, WI, USA) according to the manufacturer's instructions. The MMP-2, Bcl-2 and FGF-2 primers were synthesized by GenScript (Nanjing, China). The sequences of the MMP-2, Bcl-2, FGF-2 and GAPDH primers were as follows: MMP-2: Sense primer 5'-GGG GGATCCGCCTCCGAAACCATGAACTT-3', antisense 5'-CCCGAA TTCTCCTGGTGAGAGATCTGGTT-3'; Bcl-2: sense 5'-GGGGGAT CCGCCTCCGAAACCATGAACTT-3', antisense 5'-CCCGAATT

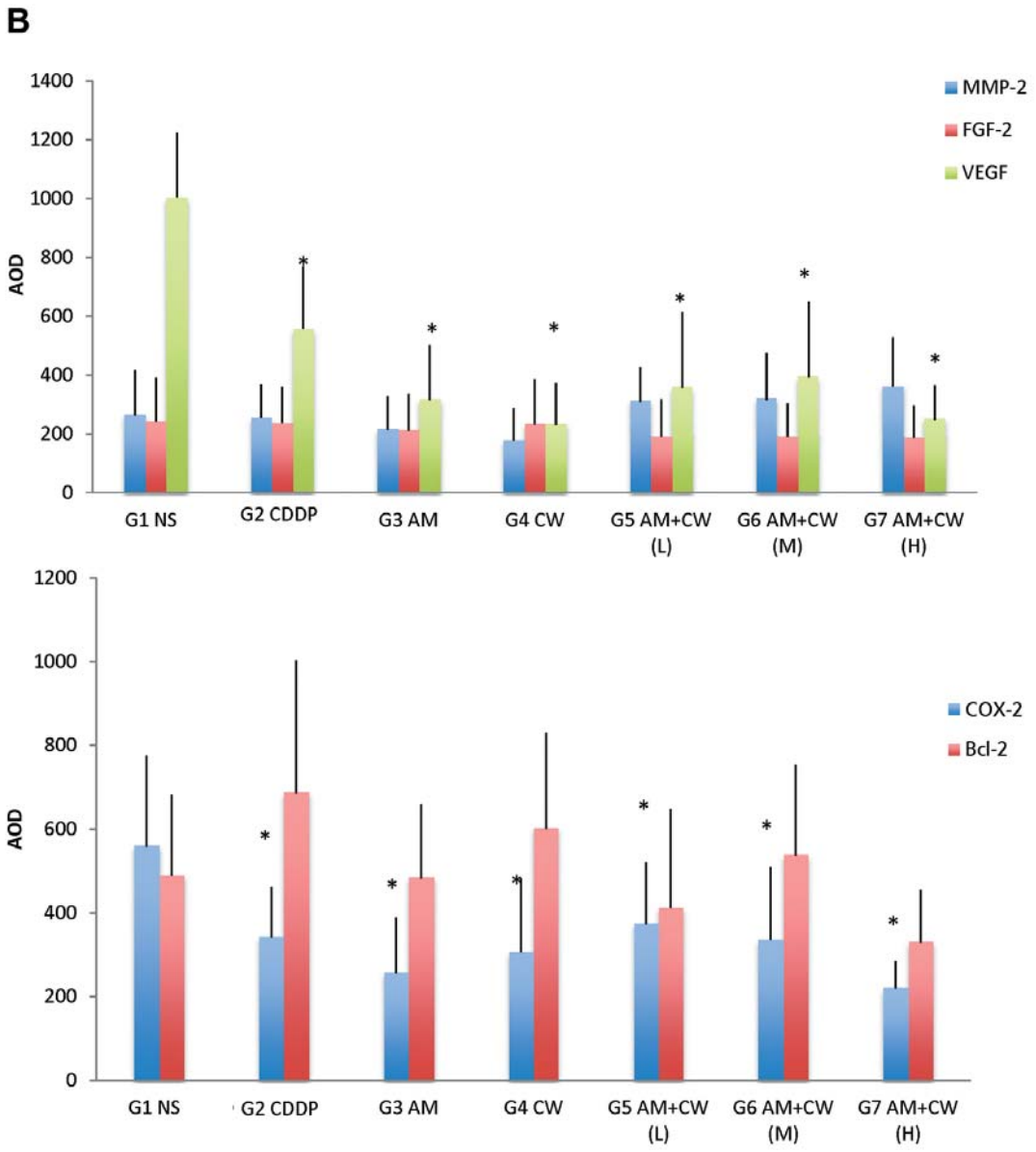

Figure 5. *Continued*

CTCCTGGTGAGAGATCTGGTT-3'; FGF-2: sense 5'-GGGGGATCC GCCTCCGAAACCATGAACTT-3', antisense 5' CCC GAATTCTCC TGGTGAGAGATCTGGTT-3'; GAPDH: sense 5'-ATC ATCCCT GCCTCTACTGG-3', antisense 5'-GTCAGGTCCACCACT GACAC-3'. RT-PCR was performed with an Access RT-PCR kit (Promega) according to the manufacturer's instructions. Each reaction contained 10 µl 5 × AMV/Tfl reaction buffer, 1 µl dNTP mix, 1 µl Tfi DNA polymerase, 1 µl AMV reverse transcriptase, 3 µl 25 mmol/l magnesium sulfate, 0.5 µg total RNA, 50 pmol of each of MMP-2, Bcl-2, FGF-2 and GAPHD primers. Reaction conditions for reverse transcription were: 48˚C for 45 min for reverse transcription; 94˚C incubation for 2 min to denature hybridized RNA/cDNA and inactivate AMV reverse transcriptase. Reaction conditions for amplification of target genes were 40 cycles of denaturing at 94˚C for 30 s; annealing at 55˚C for 30 s; extension at 68˚C for 90 s; and final extension at 68˚C for 7 min. PCR products were analyzed on 2% agarose gels and stained with ethidium bromide. Gels were scanned and images were analyzed using UNSCANIT software (SilK Scientific, Orem, UT, USA). MMP-2, Bcl-2-FGF-2, and GAPHD expression ratios were calculated.

Statistical analysis. Data are expressed as means ± SD, and were analyzed using SPSS16.0 software (SPSS inc., Chicago, Illinois, USA). Two or multiple group comparisons were performed using the Student's *t*-test or ANOVA. Fisher's exact test was used to compare the difference in the incidence of metastasis. A value of $p \leq 0.05$ was regarded as statistically significant.

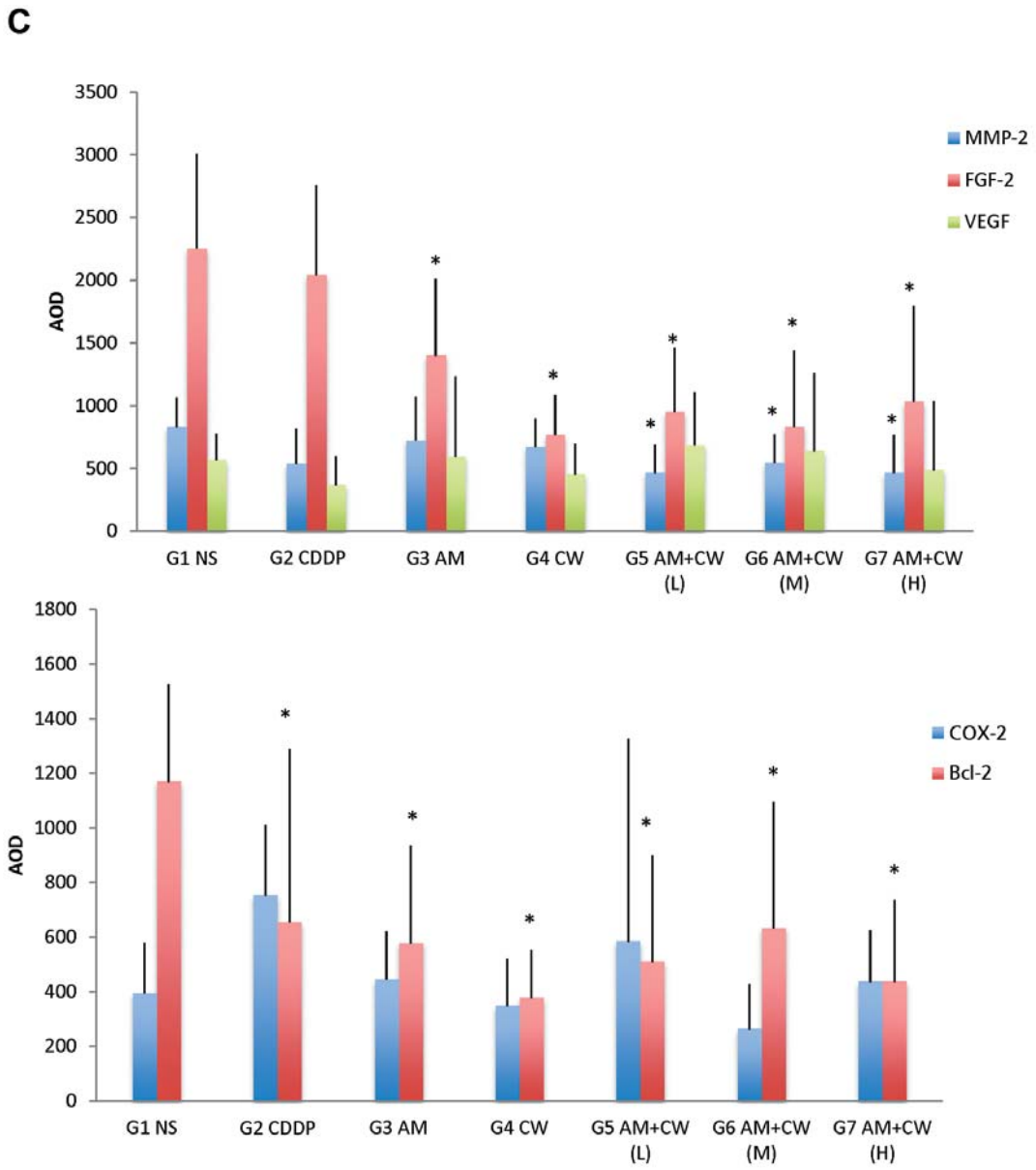

Figure 5. *Effect of Astragalus membranaceus (AM), Curcuma wenyujin (CW), normal saline (NS), cisplatinum (CDDP), and low- (L), medium- (M), or high-dose (H) AM+CW on tumor matrix metalloproteinase 2 (MMP-2), vascular endothelial growth factor (VEGF), fibroblast growth factor 2 (FGF-2), B-cell lymphoma 2 (Bcl-2) and cyclooxygenase 2 (Cox-2). Protein expression was analyzed by immunohistochemical staining and quantitated by average optical density (AOD). A: Stage I tumors; B: Stage II tumors; C: Stage III tumors. *p<0.05, when compared with untreated control; #p<0.05, when compared with CDDP-treated and other AM- and CW-treated mice.*

Results

Staging of orthotopic nude mouse model of human ovarian cancer. As shown in Figure 1, the tumor at day 24 after tumor implantation met the criteria for Stage I, in which tumor was found only at the primary site and within the intact capsule of the ovary. The average tumor volume was approximately 70 mm^3. The tumor at day 53 after implantation met the criteria for Stage II, in which tumor was found only at the primary site with invasion to surrounding fat tissues. The average tumor volume was approximately 250 mm^3. The tumor at day 78 after tumor implantation met the criteria for Stage III, in which tumor was found in multiple sites and had metastasized to other pelvic tissues and abdominal lymph nodes.

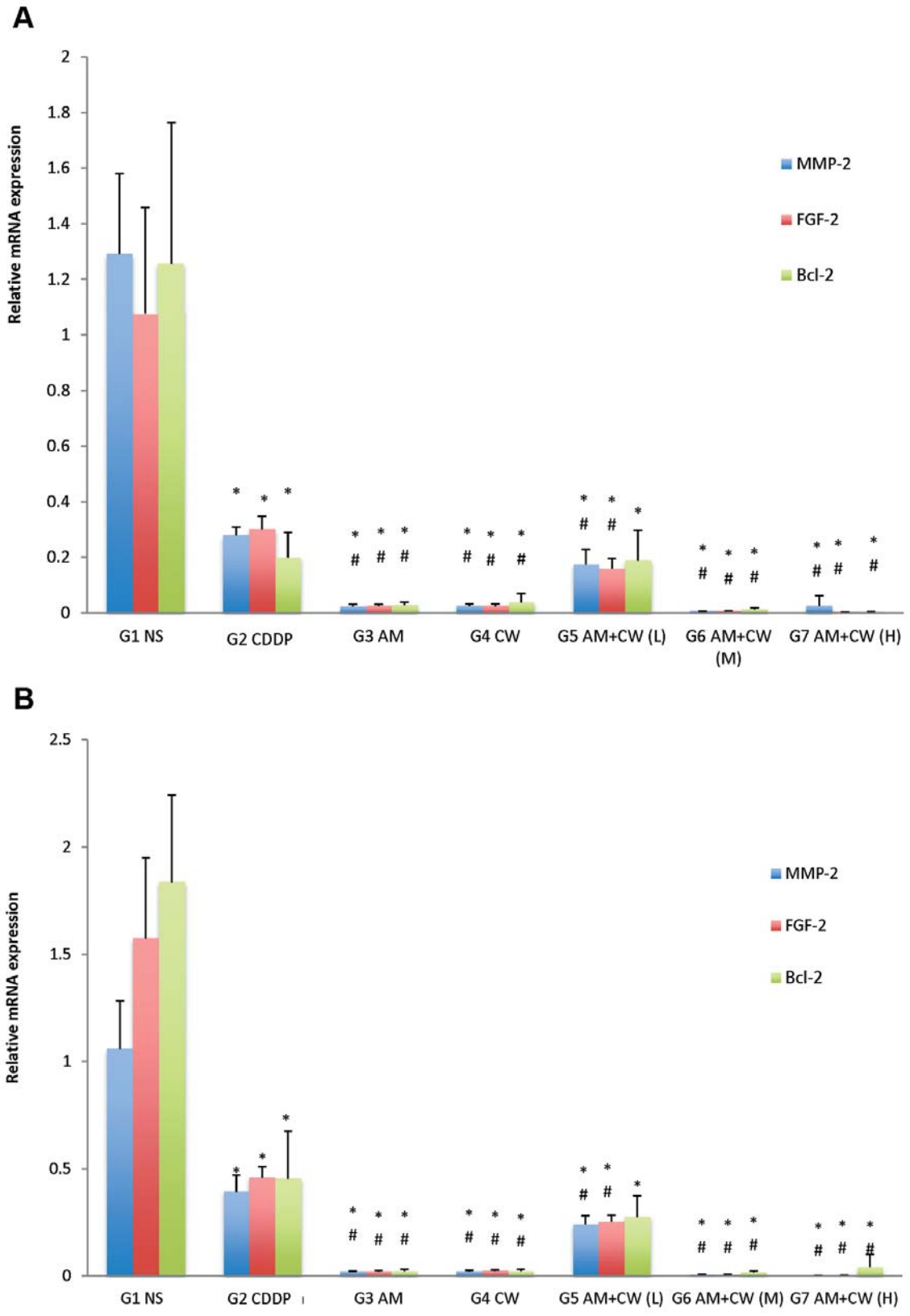

Figure 6. *Continued*

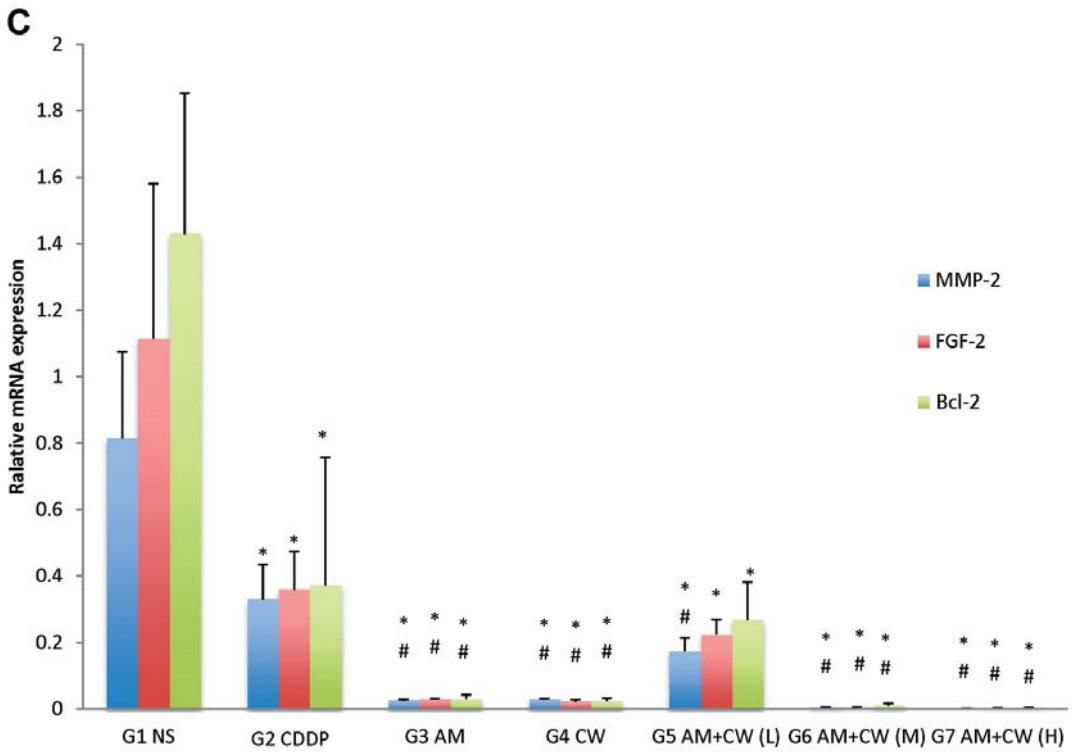

Figure 6. *Effect of Astragalus membranaceus (AM), Curcuma wenyujin (CW), normal saline (NS), cisplatinum (CDDP), AM, CW, or low- (L), medium- (M), or high (H)-dose AM+CW on tumor matrix metalloproteinase 2 (MMP-2), fibroblast growth factor 2 (FGF-2), and B-cell lymphoma 2 (Bcl-2) mRNA expression. Expression of MMP-2, FGF-2 and Bcl-2 mRNA was analyzed with the reverse transcription-polymerase chain reaction assay and quantitated by relative mRNA expression. A: Stage I tumors, B: Stage II tumors; C: Stage III tumors. *p<0.05 when compared with untreated controls; #p<0.05, when compared with cisplatinum (CDDP)-treated mice.*

Effect of AM and CW on primary tumor growth. The Stage I study was initiated on day 24 after tumor implantation. As shown in Figure 2A and B, tumor growth was significantly reduced by high-dose AM plus CW, and CDDP compared to the untreated control at all time points in the course of treatment ($p<0.05$). Efficacy of AM and medium-dose AM+CW were observed only at day 41 after tumor implantation ($p<0.05$). As shown in Figure 2C, final tumor weights were significantly reduced compared to the untreated control; by CDDP; AM; medium-dose AM plus CW; and high-dose AM plus CW ($p<0.05$). High-dose AM plus CW had significantly more efficacy than other treatment groups with regard to tumor volume and final tumor weight ($p<0.05$). No significant tumor volume and final weight reduction were found with high-dose CW or low-dose AM plus CW compared to the untreated control ($p>0.05$).

None of the CDDP-, AM-, CW- and combination-treated groups showed significant reduction of tumor volume and final weight as compared to untreated control in Stage II ($p>0.05$) (Figure 3), or Stage III tumors ($p>0.05$) (Figure 4).

Effect of AM and CW on metastasis. Fewer total metastases were observed in all CDDP- , AM-, CW- and combination-treated mice compared to untreated controls in Stage I and III (Table I) tumors at autopsy, although statistical significance was not achieved ($p>0.05$).

Effect of AM and CW on the expression of tumor angiogenesis and apoptosis-related genes. In Stage I tumors, the protein expression of MMP-2, FGF-2, VEGF and Cox-2 was significantly reduced in mice treated with AM, CW, and all doses of AM plus CW, compared to untreated controls ($p<0.05$). CDDP-treated mice showed significantly reduced MMP-2, VEGF and Cox-2 protein expression compared to untreated control mice ($p<0.05$). MMP-2, FGF-2, VEGF, and Cox-2 protein expression levels were more greatly reduced in mice treated with AM plus CW than other treatment groups ($p<0.05$). Bcl-2 protein expression in the tumor was not affected in any of the treated groups ($p>0.05$) (Figure 5).

In Stage II tumors, only VEGF and Cox-2 protein expression was significantly reduced in treated groups compared to untreated controls ($p<0.05$). MMP-2, FGF-2,

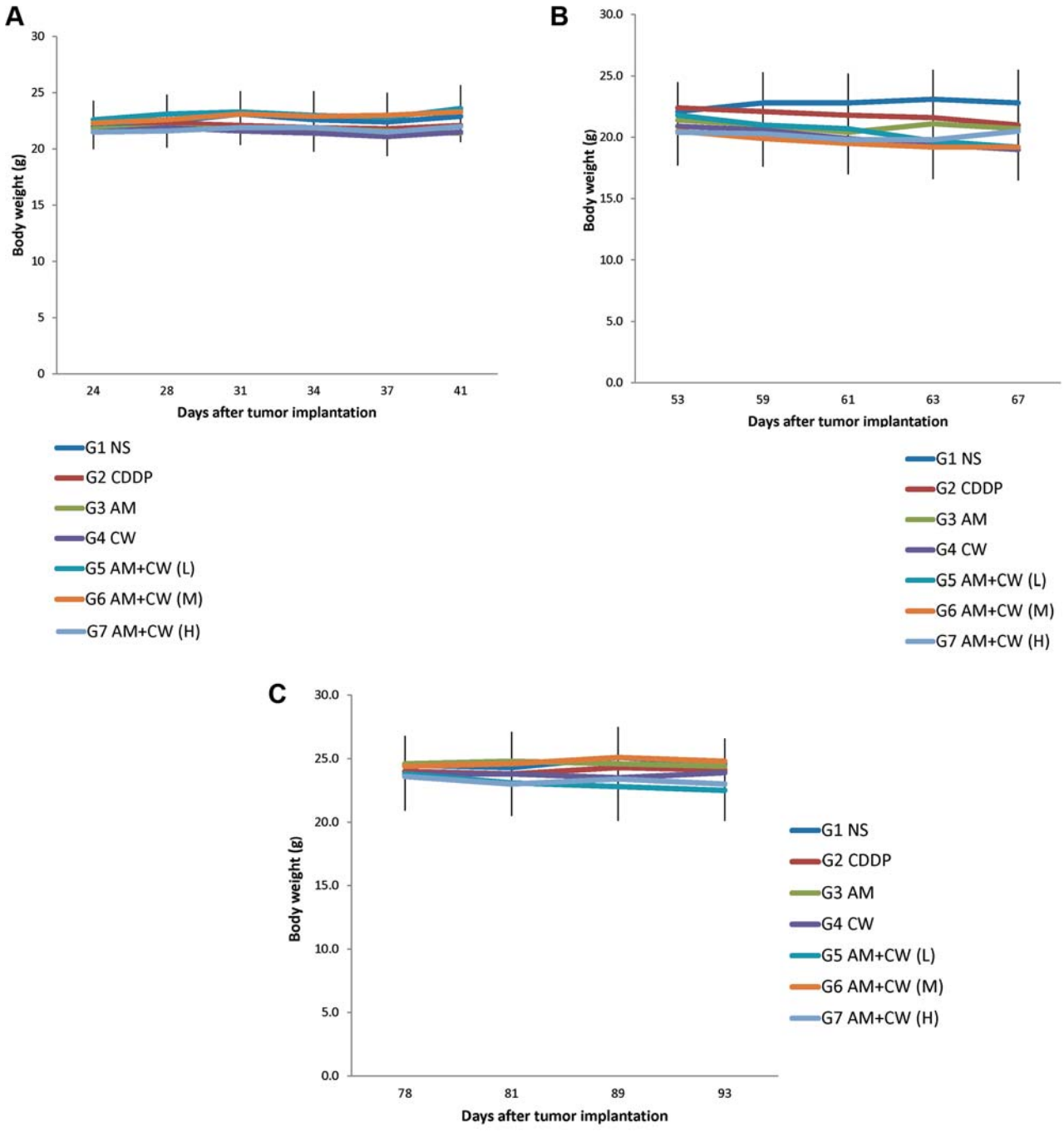

Figure 7. *Effect of Astragalus membranaceus (AM) and Curcuma wenyujin (CW) on mouse body weight in the orthotopic human HO-8910-RFP ovarian cancer mouse model. A: Stage I tumors; B: Stage II tumors; C: Stage III tumors. No significant body weight loss was observed in any AM-and CW-treated mice.*

and Bcl-2 protein expression was not affected in any treated group ($p>0.05$) (Figure 5).

In Stage III tumors, only FGF-2 and Bcl-2 protein expression was significantly reduced in treated groups compared to untreated controls ($p<0.05$). MMP-2 expression was only significantly reduced in the three AM and CW combination groups compared to untreated controls ($p<0.05$). Cox-2 and VEGF protein expression was not affected in any treated group ($p>0.05$) (Figure 5).

As shown in Figure 6, all treatments of Stage I, II, and III tumors significantly down-regulated the expression of MMP-2, Bcl-2 and FGF-2 mRNA compared with untreated controls

($p<0.05$). The expression of MMP-2, Bcl-2 and FGF-2 mRNA was significantly reduced by AM, CW, medium-dose AM plus CW, and high-dose AM plus CW more than CDDP ($p<0.05$).

Body weight and toxicity. Clinical observation and body weight measurement of animals during the study were performed to assess toxicity of AM and CW treatments. No physical or behavioral signs that indicated adverse effects due to the treatments were observed in any treatment group in mice with Stage I, II, and III tumors. As shown in Figure 7, stable body weight in all treated groups indicated no obvious toxicity.

Discussion

This study is the first to evaluate the efficacy of AM and CW in different stages of ovarian cancer in an orthotopic tumor mouse model. We demonstrated efficacy of the AM and CW combination in Stage I ovarian tumors. Suppression of angiogenesis- and apoptosis-related genes such as FGF-2, VEGF, MMP-2 and Cox-2 may be one of the mechanisms involved in the AM- and CW-induced inhibition of growth in the Stage I ovarian tumors. As the tumors progressed, they became treatment-resistant, similar to the clinical situation, further demonstrating the utility of the model and the need for agents active in advanced-stage ovarian cancer, such as bacterial therapy (3).

The present study is another example of the use of orthotopic mouse models and fluorescent proteins to determine the efficacy of TCM herbal mixtures (35-39).

Such studies with clinically-relevant mouse models with facile imaging capability are an important step in establishing the scientific basis of TCM.

Conflicts of Interest

None of the Authors have any conflict of interest in regard to this study.

Acknowledgements

This work was supported by grants from National Natural Science Foundation of China 81073072 and 81373990 and the Priority Academic Program Development of Jiangsu Higher Education Institutions.

References

1 Fu X and Hoffman RM: Human ovarian carcinoma metastatic models constructed in nude mice by orthotopic transplantation of histologically intact patient specimens. Anticancer Res *13*: 283 286, 1993.

2 Kiguchi K, Kubota T, Aoki D, Udagawa Y, Yamanouchi S, Saga M, Amemiya A, Sun FX, Nozawa S, Moossa AR, Hoffman RM: A patient-like orthotopic implantation nude mouse model of highly metastatic human ovarian cancer. Clin Exp Metastasis *16*: 751-756, 1998.

3 Matsumoto Y, Miwa S, Zhang Y, Hiroshima Y, Yano S, Uehara F, Yamamoto M, Toneri M, Bouvet M, Matsubara H, Hoffman R, M, and Zhao M: Efficacy of tumor-targeting Salmonella typhimurium A1-R on nude mouse models of metastatic and disseminated human ovarian cancer. J Cell Biochem *115*: 1996-2003, 2014.

4 Yang M, Baranov E, Wang J-W, Jiang P, Wang X, Sun F-X, Bouvet M, Moossa AR, Penman S, and Hoffman RM:Direct external imaging of nascent cancer, tumor progression, angiogenesis, and metastasis on internal organs in the fluorescent orthotopic model. Proc Natl Acad Sci USA *99*: 3824-3829, 2002.

5 Hoffman RM: The multiple uses of fluorescent proteins to visualize cancer *in vivo*. Nature Reviews Cancer *5*: 796-806, 2005.

6 Purmova J, Opletal L: Phytotherapeutic aspects of diseases of the cardiovascular system. 5. Saponins and possibilities of their use in prevention and therapy. Ceská a Slovenská farmacie *44*: 246-251, 1995.

7 Chen XJ, Meng D, Feng L, Bian YY, Li P, Yang D, Cao KJ, Zhang JN: Protective effect of astragalosides on myocardial injury by Isoproterenol in SD rats. Am J Chinese Med *34*: 1015-1025, 2006.

8 Yesilada E, Bedir E, Calis I, Takaishi Y, Ohmoto Y: Effects of triterpene saponins from Astragalus species on *in vitro* cytokine release. J Ethnopharmacology *96*: 71-77, 2005.

9 Wang YP, Li XY, Song CQ, Hu ZB: Effect of astragaloside IV on T-, B-lymphocyte proliferation and peritoneal macrophage function in mice. Acta Pharmacol Sin *23*: 263-266, 2002.

10 Lai PK, Chan JY, Cheng L, Lau CP, Han SQ, Leung PC, Fung KP, Lau CB: Isolation of anti-infl ammatory fractions and compounds from the root of *Astragalus membranaceus*. Phytother Res *27*: 581-587, 2013.

11 Ren J, Xu HJ, Cheng H, Xin WQ, Chen X, Hu K: Synthesis and antitumor activity of Formononetin nitrogen mustard derivatives. Eur J Med Chem *54*: 175-187, 2012.

12 Tin, MM, Cho CH, Chan K, James AE, Ko JK: *Astragalus* saponins induce growth inhibition and apoptosis in human colon cancer cells and tumor xenograft. Carcinogenesis *28*: 1347-1355, 2007.

13 Law PC, Auyeung KK, Chan LY, Ko JK: *Astragalus* saponins down-regulate vascular endothelial growth factor under cobalt chloride-stimulated hypoxia in colon cancer cells. BMC Complement Altern Med *12*: 160-167, 2012.

14 Liu X, Yang Y, Zhang X, Xu S, He S, Huang W, Roberts MS: Compound *Astragalus* and *Salvia miltiorrhiza* extract inhibits cell invasion by modulating trans¬forming growth factor-beta/Smad in HepG2 cell. J Gastroenterol Hepatol *25*: 420-426, 2010.

15 Cui R, He J, Wang B, Zhang F, Chen G, Yin S, Shen H. Suppressive effect of *Astragalus membranaceus* Bunge on chemical hepatocarcinogenesis in rats. Cancer Chemother Pharmacol *51*: 75-80, 2003.

16 Ye Y, Hou R, Chen J, Mo L, Zhang J, Huang Y, Mo Z: Formononetin induced apoptosis of human prostate cancer cells through ERK1/2 mitogen-activated protein kinase inactivation. Horm Metab Res *44*: 263-267, 2012.

17 Chen J, Sun L: Formononetin-induced apoptosis by activation of Ras/p38 mitogen-activated protein kinase in estrogen receptor-positive human breast cancer cells. Horm Metab Res *44*: 943-948, 2012.

18 Na D, Liu FN, Miao ZF, Du ZM, Xu HM: Astragalus extract inhibits destruction of gastric cancer cells to mesothelial cells by anti-apoptosis. World J Gastroenterol *15*: 570-577, 2009.

19 Chen J, Zeng J, Xin M, Huang W, Chen X: Formononetin induces cell cycle arrest of human breast cancer cells *via* IGF1/PI3K/AKT pathways *in vitro* and *in vivo*. Horm Metab Res *43*: 681-686, 2011.
20 Lai EY, Chyau CC, Mau JL, Chen CC, Lai YJ, Shih CF, Lin LL: Antimicrobial activity and cytotoxicity of the essential oil of *Curcuma zedoaria*. Am J Chin Med *32*: 281-290, 2004.
21 Makabe H, Maru N, Kuwabara A, Kamo T, Hirota M: Antiinflammatory sesquiterpenes from *Curcuma zedoaria*. Nat Prod Res *20*: 680-685, 2006.
22 Tohda C, Nakayama N, Hatanaka F, Komatsu K: Comparison of anti-inflammatory activities of six curcuma rhizomes: a possible curcuminoid-independent pathway mediated by *Curcuma phaeocaulis* extract. Evid Based Complement Alternat Med *3*: 255-260, 2006.
23 Park SD, Jung JH, Lee HW, Kwon YM, Chung KH, Kim MG, Kim CH: Zedoariae rhizoma and curcumin inhibits platelet-derived growth factor-induced proliferation of human hepatic myofibroblasts. Int Immunopharmacol *5*: 555-569, 2005.
24 Xiao Y, Yang FQ, Li SP, Hu G, Lee SM, Wang YT: Essential oil of *Curcuma wenyujin* induces apoptosis in human hepatoma cells. World J Gastroenterol *14*: 4309-4318, 2008.
25 Syu WJ, Shen CC, Don MJ, Ou JC, Lee GH, Sun CM: Cytotoxicity of curcuminoids and some novel compounds from *Curcuma zedoaria*. J Nat Prod *61*: 1531-1534, 1998.
26 Dong R, Chen X, Wu T, :Liu GJ: Elemene for the treatment of lung cancer. Cochrane Database Syst Rev *2007*: CD006054.
27 Zhou R, Xu L, Ye M, Liao M, Du D, Chen H: Formononetin inhibits migration and invasion of MDA-MB-231 and 4T1 breast cancer cells by suppressing MMP-2 and MMP-9 through PI3K/AKT signaling pathways. Horm Metab Res *46*: 753-760, 2014.
28 Lim CB, Ky N, Ng HM, Hamza MS, Zhao Y: *Curcuma wenyujin* extract induces apoptosis and inhibits proliferation of human cervical cancer cells *in vitro* and *in vivo*. Integrative Cancer Therapies *9*: 36-49, 2010.
29 Sun XY, Zheng YP, Lin DH, Zhang H, Zhao F, Yuan CS: Potential anticancer activities of furanodiene, a sesquiterpene from *Curcuma wenyujin*. Am J Chinese Med *37*: 589-596, 2009.
30 Zhong Z, Dang Y, Yuan X, Guo W, Li Y, Tan W, Cui J, Lu J, Zhang Q, Chen X, Wang Y: Furanodiene, a natural product, inhibits breast cancer growth both *in vitro* and *in vivo*. Cell Physiol Biochem *30*: 778-790, 2012.
31 Tang D, Zang WH, Feng HH: The experimental study of proliferation inhibition and apoptosis induction of serum with different curcuma in ovarian cancer cell HO-8910. Lishizhen Medicine and Materia Medica Research *24*: 2313-2315, 2013.
32 Hoffman RM: Orthotopic metastatic mouse models for anticancer drug discovery and evaluation: a bridge to the clinic. Investigational New Drugs *17*: 343-359, 1999.
33 Edge SB, Byrd DR, Compton CC, Fritz AG, Greene FL, Trotti A. *AJCC Cancer Staging Manual*. 7th ed. New York, NY: Springer-Verlag; 493-506. 2010.
34 Pecorelli S, Odicino F, Maisonneuve P, *et al*. Carcinoma of the ovary. FIGO annual report on the results of treatment in gynaecological cancer. J Epidemiol Biostat *3*: 75-102, 1998.
35 Wang M, Zhang X, Xiong X, Yang Z, Sun Y, Yang Z, Hoffman RM, Liu Y. Efficacy of the Chinese Traditional Medicinal Herb Celastrus orbiculatus Thunb on human hepatocellular carcinoma in an orthotopic fluorescent nude mouse model. Anticancer Res 32: 1213-1220, 2012.
36 Hu M, Zhao M, An C, Yang M, Li Q, Zhang Y, Suetsugu A, Tome Y, Yano S, Fu Y, Hoffman RM, Hu K. Real-time imaging apoptosis induction of human breast cancer cells by the traditional Chinese medicine herb tubeimu. Anticancer Res *32*: 2509-2514, 2012.
37 Zhang Y, Zhang N, Su S, Hoffman RM, Zhao M. *Salmonella typhimurium* A1-R tumor targeting in immunocompetent mice is enhanced by a traditional Chinese medicine herbal mixture. Anticancer Res *33*: 1837-1843, 2013.
38 Zhang L, Wu C, Zhang Y, Liu F, Zhao M, Bouvet M, Hoffman RM. Efficacy comparison of traditional Chinese medicine LQ *versus* gemcitabine in a mouse model of pancreatic cancer. J. Cell. Biochem *114*: 2131-2137, 2013.
39 Zhang L, Wu C, Zhang Y, Liu F, Wang X, Zhao M, Hoffman RM. Comparison of efficacy and toxicity of Traditional Chinese Medicine (TCM) herbal mixture LQ and conventional chemotherapy on lung cancer metastasis and survival in mouse models. PLoS One *9*: e109814, 2014.

Received March 10, 2015
Revised March 31, 2015
Accepted April 3, 2015